Time evolution of the Wigner function in discrete quantum phase space for a soluble quasi-spin model

2000 J. Phys. A: Math. Gen. 33 2799

(http://iopscience.iop.org/0305-4470/33/14/313)

J. Phys. A: Math. Gen. **33** (2000) 2799–2816. Printed in the UK PII: S0305-4470(00)09926-1

Time evolution of the Wigner function in discrete quantum phase space for a soluble quasi-spin model

D Galetti and M Ruzzi

Instituto de Física Teórica, Universidade Estadual Paulista, Rua Pamplona 145, 01405-900 São Paulo, S P, Brazil

Received 26 November 1999

Abstract. The discrete phase space approach to quantum mechanics of degrees of freedom without classical counterparts is applied to the many-fermions/quasi-spin Lipkin model. The Wigner function is written for some chosen states associated to discrete angle and angular momentum variables, and the time evolution is numerically calculated using the discrete von Neumann–Liouville equation. Direct evidences in the time evolution of the Wigner function are extracted that identify a tunnelling effect. A connection with a $SU(2)$-based semiclassical continuous approach to the Lipkin model is also presented.

(Some figures in this article appear in black and white in the printed version.)

1. Introduction

The quantum phase space continuous descriptions of physical systems have deserved attention over the years and the literature shows the increasing interest in this area [1–7]. On the other hand, paralleling the well known continuous treatment, discrete phase space descriptions have also been introduced and widely discussed which account for quantum degrees of freedom without classical counterpart [8–16].

In what concerns the discrete phase space approach, the mapping of operators acting over finite-dimensional state spaces, associated to one such degree of freedom, onto functions of integers, has been shown to be obtained as the discrete analogue to the continuous Weyl–Wigner decomposition of operators onto an operator basis. In particular, the density operator describing the physical system state can also be mapped, which still deserves to be called a Wigner function, in the same form as the other operators; in this case it is only defined over the sites of a finite lattice characterizing the discrete finite phase space.

Among the various physical situations for which the system state space is finite-dimensional, and therefore the discrete phase space description can be suitably used, we want to distinguish the family of problems that can be modelled in terms of Hamiltonians dealing with angular momenta/spins or quasi-spins. For example, the quantum systems of mesoscopic magnets composed of a small number of spins can be used as a remarkable example of such a system [17]. Another field of recent interest which also requires this kind of treatment is quantum state tomography that makes explicit use of discrete Wigner functions [18]. In a general context it is also important to note that a discrete phase space approach for $SU(2)$ and $SU(1, 1)$ systems has already been proposed and developed in the past [19].

As is well known, all these systems must behave according to quantum mechanics, and once the degrees of freedom of such systems have been sieved, for each of them separately we

0305-4470/00/142799+18$30.00

can construct the operator basis with which the construction of the corresponding discrete quantum phase space representation is then available through the mapping procedure as previously presented in [9].

The discrete mapped expression of a model Hamiltonian, associated to one of the degrees of freedom, can be directly used in order to obtain the time evolution of the Wigner function through the use of the discrete mapped von Neumann–Liouville equation. Such a formalism describing the time evolution of the discrete Wigner function has been already proposed [20], and is based on the existence of a discrete dynamical bracket which is a discrete analogue of the continuous Moyal bracket. In this scheme, the discrete quantum Liouvillian governing the time evolution is obtained as the discrete mapped expression of the commutator of the Hamiltonian. In fact, in that work we have developed the series consisting of the iterated action of the Liouvillian over the initial discrete Wigner function which gives its time evolution, and, as a direct application, we have used it in the simple case of a general magnetic moment precession in a time-independent external magnetic field. Due to the simplicity of that model Hamiltonian, the density propagator can be analytically obtained and reoccurence times can be directly discussed [20].

In this paper we apply the formalism presented previously to a solvable model whose Hamiltonian, although simple, presents some interesting features, namely the Lipkin–Meshkov–Glick quasi-spin model (LMGM) [21]. This originally many-fermion Hamiltonian can be also described as a quasi-spin model, and, in this form, it is composed of a pure J_z term—giving an equally spaced energy spectrum—plus an interaction term, controlled by a strength constant χ, which couples the J_z eigenstates. The underlying $SU(2)$ structure of this Hamiltonian can be clearly verified. Our attention here will be focused only on the ground state finite multiplet (for a finite number of fermions) of this model which will play the role of our finite-dimensional space of interest. For this space, the mapping procedure allowing for the discrete phase space representation can be directly implemented, and the discrete Liouvillian can be obtained in such a way that the series defining the time propagator for the density can be calculated.

As is well known, in the Lipkin model, for a given number of fermions/quasi-spins N_p, as χ increases, the two lowest energy levels show a trend to collapse as a single degenerate state. For $N_p \to \infty$, this effect gives rise to a ground state phase transition ($T = 0$) characterized by the appearance of a degenerated state for $\chi_c = 1$. This interesting aspect of this model has also been long discussed in the semiclassical context mainly within the use of $SU(2)$ continuous coherent states [22–25].

Our primary aim here, however, is the study of the time evolution of the discrete Wigner function written in terms of discrete angle and angular momentum variables. First of all, we will carry out the time evolution for a small number of fermions/quasi-spins in order to treat a quantum mesoscopic system. In this case we show that the time-evolved discrete Wigner function can give direct information about the behaviour of the system. In particular, we show that the time evolution of the marginal distribution associated to the discrete angle variable, obtained from a trace operation on the Wigner function, is the best way to search for clues indicating the change of behaviour of the system as we increase the coupling strength χ (while the lowest energy levels almost collapse). The marginal distributions associated to the angular momentum are much less elucidative and will not be discussed in detail.

Observing the time evolution of the angle distribution function we see that it reveals the appearance of secondary peaks which strongly suggests reflections and transmissions through a potential barrier. Although the original LMGM Hamiltonian does not explicitly exhibit such a potential function in terms of an angle variable, its discrete phase space mapped version is in fact written in terms of discrete angular and angle variables. Motivated by these results, and in order to discuss a semiclassical limit of our treatment, we also discuss a connection between our

originally discrete phase space description and a particular case of the semiclassical coherent-state-based continuous treatments of the LMGM. In this way, we show how a potential function of a discrete angle variable can be extracted from our formulation such that its behaviour for $N_p \to \infty$ coincides with the continuous semiclassical one.

This paper is organized as follows. Section 3 presents a brief review of the main aspects of the LMG model. In section 3 the Liouvillian for the LMGM is presented and in section 3.1. the equations governing the time evolution of the discrete Wigner function are discussed and the results are presented. A discussion of a connection between our description and a semiclassical treatment of the LMGM, through the introduction of a potential function of a discrete angle variable, is presented in section 4. Finally, section 5 is devoted to our conclusions.

2. The Lipkin model

The standard Lipkin–Meshkov–Glick model [21] has been widely discussed in the past so here we will only outline its main features.

In this model a collection of N_p (here considered an even number) fermions is distributed in two N_p-fold degenerate levels separated by an energy ϵ. The degenerate states within each level are labelled by a quantum number q, which assumes values between 1 and N_p, and σ which is equal to $+1(-1)$ for the higher (lower) level. The Hamiltonian of the model is given by

$$H = \frac{\epsilon}{2}\sum_{q,\sigma}\sigma a^{\dagger}_{q,\sigma}a_{q,\sigma} + \frac{V}{2}\sum_{q,q',\sigma} a^{\dagger}_{q,\sigma}a^{\dagger}_{q',\sigma}a_{q',-\sigma}a_{q,-\sigma}. \tag{1}$$

The model, besides being soluble, can be put in a more suitable form to treat collective excitations of the fermions system if we realize that a subjacent algebraic struture can be identified within this Hamiltonian. If we introduce the quasi-spin operators

$$J_+ = \sum_q a^{\dagger}_{q,+1}a_{q,-1} \tag{2}$$

$$J_- = \sum_q a^{\dagger}_{q,-1}a_{q,+1} \tag{3}$$

$$J_z = \tfrac{1}{2}\sum_{q,\sigma}\sigma a^{\dagger}_{q,\sigma}a_{q,\sigma} \tag{4}$$

we see that the Lipkin Hamiltonian can then be written as

$$H = \epsilon J_z + \frac{V}{2}(J_+^2 + J_-^2). \tag{5}$$

It is then clear that the J_z term gives half the difference of the number of particles in the upper and lower levels, while the second term is associated to the interaction between a pair of particles in the same energy level, and which scatters this pair to the other level without changing the quantum number q of each particle.

It is also direct to verify that these new operators indeed obey the standard $SU(2)$ commutation relations, namely,

$$[J_+, J_-] = 2J_z \tag{6}$$

$$[J_z, J_\pm] = \pm J_\pm. \tag{7}$$

It is useful to rewrite that Hamiltonian in such a way to scale the interaction term to the particle number while measuring the energy in terms of ϵ,, i.e.,

$$H_L = \frac{H}{\epsilon} = J_z + \frac{\chi}{2N_p}(J_+^2 + J_-^2) \tag{8}$$

with $\chi = N_p V/\epsilon$.

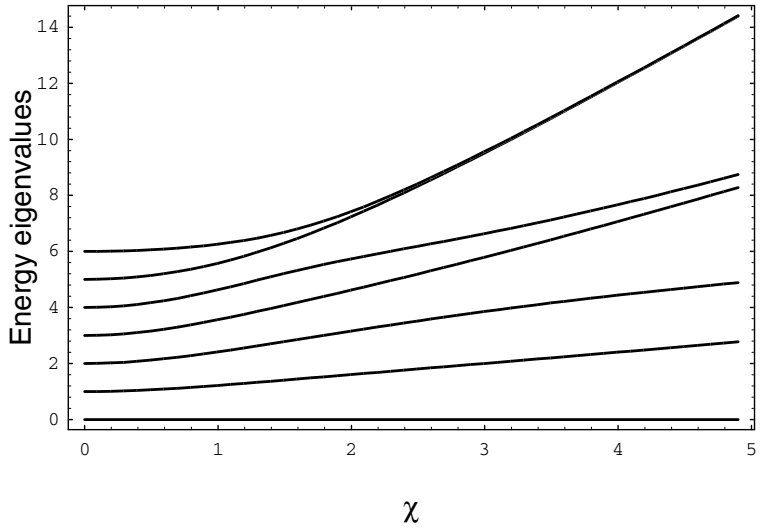

Figure 1. Positive energy spectrum for $N_p = 12$ as a function of the parameter χ. The negative energy spectrum is obtained by taking $-E_k$.

With the Hamiltonian written in terms of these quasi-spin operators, one can immediately see that, since $[H, J^2] = 0$, it can be diagonalized within each multiplet labelled by the eigenvalues of J^2 and J_z, which accounts for the soluble character of the associated quantum dynamical problem. Each multiplet is $(2J + 1)$-dimensional. Here we also note that the ground state belongs to the multiplet $J = \frac{N_p}{2} = \max J_z$, with eigenvalues $\frac{N_p}{2}(\frac{N_p}{2}+1)$ and $-\frac{N_p}{2}$ respectively.

Furthermore, from symmetry considerations, we immediately see that the model presents some discrete conserved quantities. The simplest constant of motion is related to the parity operator

$$\Pi = \exp(\mathrm{i}\pi J_z) \tag{9}$$

indicating that the Hamiltonian matrix, in the J_z representation, breaks into two disjoint blocks involving only even and odd eigenvalues of J_z respectively. A second interesting property of the energy spectrum is revealed by the fact that the Hamiltonian anticommutes with the operator

$$R = \exp\left(\mathrm{i}\frac{\pi}{2}J_z\right)\exp(\mathrm{i}\pi J_y) = \sum_{m=-N_p}^{N_p} |-m\rangle(-1)^{N_p+m}\langle m|. \tag{10}$$

This operator corresponds to a rotation of the angular momentum quantization frame by the Euler angles $(-\frac{\pi}{2}, \pi, 0)$, thus transforming $H \to -H$. As a result of this anticommutation property we verify that if $|E_j\rangle$ is an energy eigenstate with eigenvalue E_j, then the state $R|E_j\rangle$ is an eigenstate of the Hamiltonian with eigenvalue $-E_j$. This symmetry property of the Hamiltonian gives rise to an energy spectrum that is symmetric about zero.

The exact solution of this Hamiltonian has long been known for different N_p values, see Lipkin [21]. Once the spectrum is obtained it is a simple task to find the energy gap, $(E_1 - E_0)/\epsilon$, which is also a very important quantity characterizing the behaviour of this model as a function of the interaction parameter χ. As an illustration of this, figure 1 shows a typical spectrum for $N_p = 12$ as a function of the parameter χ.

3. Discrete phase space description

We will consider hereafter the ground state multiplet characterized by the states $|\frac{N_p}{2}, m\rangle$, where m assumes values $-\frac{N_p}{2} \leqslant m \leqslant \frac{N_p}{2}$, and the dimension of the corresponding state space is therefore $N = N_p + 1$. Hereafter we will use $\hbar = 1$.

As already performed in our previous papers [9, 13, 26], it is possible to identify the states $|\frac{N_p}{2}, m\rangle$ as the eigenstates of the Schwinger unitary operator U [27], i.e.,

$$U \left| \frac{N_p}{2}, m \right\rangle = \exp\left(\frac{2\pi \mathrm{i}}{N} m\right) \left| \frac{N_p}{2}, m \right\rangle \tag{11}$$

so that we can hereafter assume $|\frac{N_p}{2}, m\rangle \equiv |u_m\rangle$. As such, we also have the complementary unitary operator [27]

$$V^s |u_m\rangle = |u_{m-s}\rangle \tag{12}$$

here $m - s$ is to be considered as $(m - s) \bmod N$.

The operator basis which allows for discrete Weyl–Wigner transformations of quantum mechanical operators O, acting on finite N-dimensional spaces, onto discrete phase space representatives, is given by [9, 13]

$$G(m, n) = \sum_{j,l} \frac{U^j V^l}{N} \exp\left[\mathrm{i}\pi\phi(j, l; N) - \frac{2\pi \mathrm{i}}{N}(mj + nl) + \mathrm{i}\frac{\pi}{N} jl\right] \tag{13}$$

where the phase $\phi(j, l; N)$ performs all the mod N arithmetics involved in the given operator basis calculations.

If we measure the energies in units of ϵ, and scale the strength of the interaction with the number of particles, i.e., if we introduce a parameter $\chi = N_p V/\epsilon$, as we did previously, one can immediately obtain the discrete Weyl–Wigner transform of the Lipkin Hamiltonian by calculating [9, 13]

$$h_L(m, n) = \frac{1}{N} \mathrm{Tr}[G^\dagger(m, n) H_L] \tag{14}$$

which reads

$$h_L(m, n) = m + \frac{\chi}{N_p} \sqrt{\left(\frac{N_p}{2} + m\right)\left(\frac{N_p}{2} + m + 1\right)\left(\frac{N_p}{2} - m\right)\left(\frac{N_p}{2} - m + 1\right)} \cos\frac{2\pi}{N} 2n. \tag{15}$$

The discrete mapped Liouville operator, which governs the time evolution of the densities in discrete quantum phase spaces, can be directly obtained from the mapped Hamiltonian since we know how to map commutators onto the discrete phase space, and its expression has already been presented [13]. Its general form is written as

$$\begin{aligned}\mathcal{L}(u, v, r, s) = 2\mathrm{i} \sum_{m,n} \sum_{a,b,c,d} \frac{h(m, n)}{N^4} \sin\left[\frac{\pi}{N}(bc - ad)\right] \exp[\mathrm{i}\pi\Phi(a, b, c, d; N)] \\ \times \exp\left\{\frac{2\pi \mathrm{i}}{N}[a(u - m) + b(v - n) + c(u - r) + d(r - s)]\right\}\end{aligned} \tag{16}$$

where $h(m, n)$ is the discrete phase space mapped expression of the Hamiltonian of the system of interest, and $\Phi(a, b, c, d; N) = -\phi(a + c + \frac{N_p}{2}, b + d + \frac{N_p}{2}; N)$. In the present case the mapped Liouvillian reads [26]

$$\mathcal{L}(u, v, r, s) = \mathcal{L}_1(u, v, r, s) + \mathcal{L}_2(u, v, r, s) \tag{17}$$

where

$$\mathcal{L}_1(u,v,r,s) = -2\mathrm{i}\sum_{m,a,c,d}\frac{m}{N^3}\sin\left(\frac{\pi}{N}ad\right)\exp[\mathrm{i}\pi\Phi(a,0,c,d;N)] \times\exp\left\{\frac{2\pi\mathrm{i}}{N}[a(u-m)+c(u-r)+d(r-s)]\right\} \tag{18}$$

and

$$\begin{aligned}\mathcal{L}_2(u,v,r,s) = \chi\sum_{m,a,c,d}\frac{g(m,N)}{N^3}\exp\left\{\frac{2\pi\mathrm{i}}{N}[a(u-m)+d(r-s)]\right\} \\ \times\Bigg(\exp\left[4\pi\mathrm{i}\frac{v}{N}+\mathrm{i}\pi\Phi(a,2,c,d;N)\right]\Bigg\{\exp\left[\frac{2\pi\mathrm{i}}{N}c(u-r+1)-\frac{\mathrm{i}\pi ad}{N}\right] \\ -\exp\left[\frac{2\pi\mathrm{i}}{N}c(u-r-1)+\frac{\mathrm{i}\pi ad}{N}\right]\Bigg\} \\ -\exp\left[-4\pi\mathrm{i}\frac{v}{N}+\mathrm{i}\pi\Phi(a,-2,c,d;N)\right] \\ \times\left\{\exp\left[\frac{2\pi\mathrm{i}}{N}c(u-r+1)+\frac{\mathrm{i}\pi ad}{N}\right]-\exp\left[\frac{2\pi\mathrm{i}}{N}c(u-r-1)-\frac{\mathrm{i}\pi ad}{N}\right]\right\}\Bigg).\end{aligned} \tag{19}$$

Here we have called

$$g(m,N) = \frac{\sqrt{(\frac{N_p}{2}+m)(\frac{N_p}{2}+m+1)(\frac{N_p}{2}-m)(\frac{N_p}{2}-m+1)}}{N_p} \tag{20}$$

for simplicity.

The first term of the Liouvillian, equation (18), corresponds to the J_z term of the Lipkin Hamiltonian, while the second term, on the other hand, describes the mixing of the J_z eigenstates induced by the presence of the J_+^2 and J_-^2 operators.

3.1. The von Neumann–Liouville dynamics in the discrete phase space

If we want to describe the von Neumann–Liouville time evolution equation for the density operator, for time-independent Hamiltonians,

$$\mathrm{i}\frac{\partial}{\partial t}\hat{\rho}(t) = [H,\hat{\rho}(t)] \tag{21}$$

in the discrete phase space representation, we will obtain the mapped expression

$$\mathrm{i}\frac{\partial}{\partial t}\rho_w(u,v;t) = \sum_{r,s}\mathcal{L}(u,v,r,s)\rho_w(r,s;t) \tag{22}$$

where $\rho_w(u,v;t)$ is the Wigner function of the system we are interested in [13]. A solution to equation (21) in the form of a series

$$\hat{\rho}(t) = \hat{\rho}(t_0)+(-\mathrm{i})(t-t_0)[H,\hat{\rho}(t_0)]+\frac{1}{2!}(-\mathrm{i})^2(t-t_0)^2[H,[H,\hat{\rho}(t_0)]]+\cdots \tag{23}$$

has its discrete phase space mapped expression written as [20]

$$\begin{aligned}\rho_w(u,v;t) = \sum_{r,s}\Bigg\{\delta^{[N]}_{r,u}\delta^{[N]}_{s,v}+(-\mathrm{i})(t-t_0)\mathcal{L}(u,v,r,s) \\ +(-\mathrm{i})^2(t-t_0)^2\sum_{x,y}\frac{1}{2!}\mathcal{L}(u,v,x,y)\mathcal{L}(x,y,r,s)+\cdots\Bigg\}\rho_w(r,s;t_0).\end{aligned} \tag{24}$$

In this form, since we are given the Liouvillian, equation (17), we can directly compute the time evolution of the Wigner function by using the series associated to the iterated application of the discrete mapped Liouville operator. It is therefore evident that the time evolution constitutes itself in a linear process of composition of sums of products of arrays characterizing the Liouvillian and the Wigner functions respectively, over the sites which define the discrete phase space. Since this scheme only involves simple operations, it can be implemented in a simple way, and, from a numerical point of view, we only have to construct the arrays defining the Liouvillian (which is the dominant time consuming part of the numerical process) and the Wigner function. Once given the Wigner function at t_0, the series will give us the propagated function at any instant of time by using equations (24) and (17).

In what concerns the system state, it is immediate to see that the two simple cases of pure states, namely $\rho(t_0) = |u_k\rangle\langle u_k|$, and $\rho(t_0) = |v_k\rangle\langle v_k|$, can be directly mapped onto the discrete phase space giving the corresponding Wigner functions, $\rho_w(m, n; t_0) = \delta^{[N]}_{m,k}$, and $\rho_w(m, n; t_0) = \delta^{[N]}_{n,k}$ respectively. In the first case, the Wigner function is a constant for the angular momenta and is independent of the angle variable, whereas the reverse occurs for the second case. Clearly these Wigner functions are normalized to N. Furthermore, as is well known, the probability distributions for the angular momentum and for the angle can be directly obtained from the Wigner function, at any instant of time, by means of a trace operation, namely,

$$L(m; t) = \sum_{n=-\frac{N_p}{2}}^{\frac{N_p}{2}} \rho_w(m, n; t) \tag{25}$$

and

$$\Theta(n; t) = \sum_{m=-\frac{N_p}{2}}^{\frac{N_p}{2}} \rho_w(m, n; t) \tag{26}$$

respectively. The angle variable is characterized by $\theta_n = \frac{2\pi}{N} n$.

In order to keep a suitable precision in the numerical calculations for the time evolution, the series defining the action of the Liouvillian over the Wigner function were truncated whenever the contributions of its terms became $\leqslant 10^{-6}$ arbitrary units. Furthermore, we have performed all the calculations with small time steps so that the series could converge within a few terms ($\sim$10 terms), and the precision was kept at a suitable level; in this way, long timescale propagations are obtained as a series of successive small ones. Each time step was considered to be a multiple of $\Delta\tau = \frac{2\pi}{N}$.

If we consider the simplest case of $\chi = 0$, that is, a pure J_z Hamiltonian, the time evolution is simply given by a Liouvillian uniquely associated to equation (18). In this case, we have already shown [20] that a peculiar time evolution occurs, leading the initial angle state to its sucessive neighbours precisely at times that are integral multiples of $\Delta\tau$. Since in this case nothing new can be added to what has been exposed there, we refrain from further discussing it here.

Using the present scheme, we have calculated the time evolution of the Wigner function for each one of the pure state cases mentioned above, namely, $\rho_w(m, n; t_0) = \delta^{[N]}_{m,k}$ and $\rho_w(m, n; t_0) = \delta^{[N]}_{n,k}$, for fixed N_p and some values of the parameter $\chi \neq 0$. Here we have always chosen $N_p = 12$ in order to study, at least in this solvable model, the behaviour of a mesoscopic quantum system. Furthermore, we have verified that—in what refers to the features indicating the change of behaviour of the system as we increase the coupling strength χ—the time evolution of the angular momentum distribution is much less elucidative than that

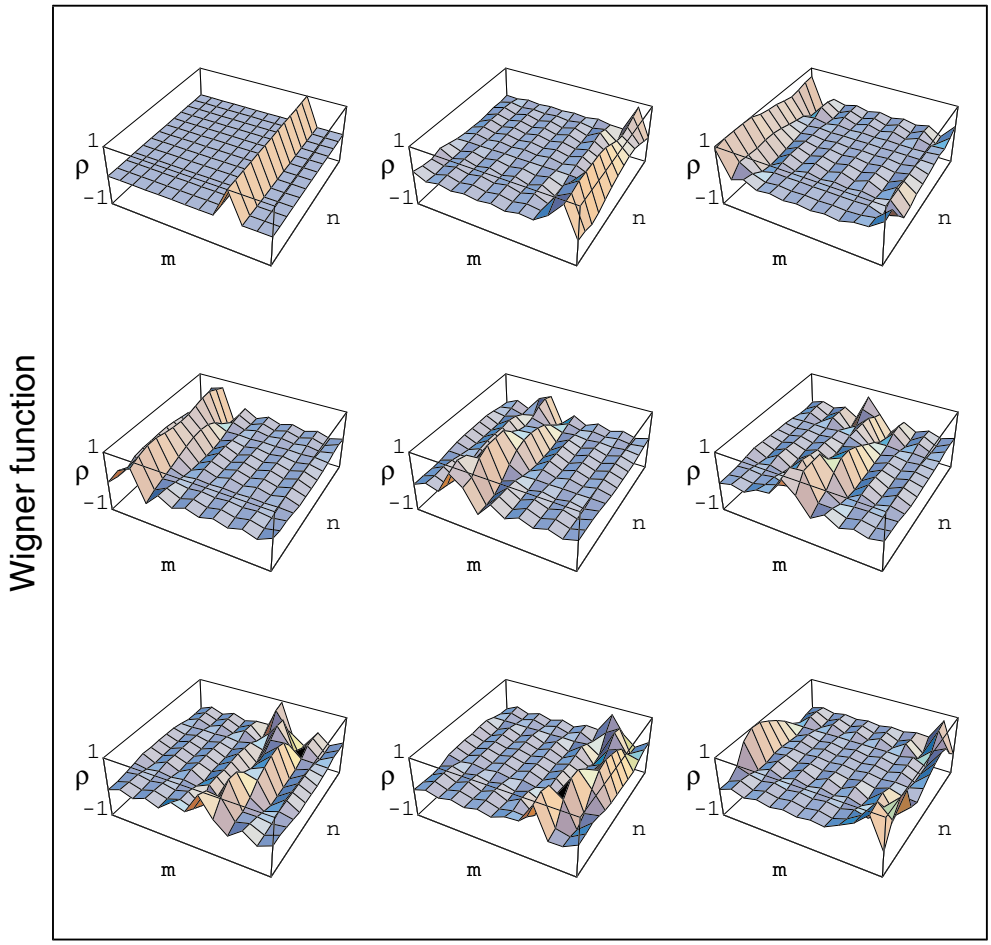

Figure 2. Time evolution of the Wigner function, $\rho_w(m,n;t_0)=\delta^{[N]}_{n,k}$ (angle sharp), for $N_p=12$ and $\chi=0.5$. The ranges of the axes are $-\frac{N_p}{2}\leqslant m,n\leqslant\frac{N_p}{2}$. The initial condition is $k=3$. The time steps are even multiples of $\Delta\tau=2\pi/N$. The solid lines are only given as a guide to the eye.

of the angle variable. Thus, we are not going to show them; instead we will only concentrate on the angle distribution.

As can be seen from figure 1, for $\chi=0.5$, the energy spectrum is almost completely dominated by the J_z term. Figure 2 shows the time sequence for the Wigner function associated to the sharp angle state, $\rho_w(m,n;t_0)=\delta^{[N]}_{n,k}$, calculated for $N_p=12$, $\chi=0.5$, and $k=3$. Figure 3 corresponds to the time evolution of the angle probability distribution as extracted from the previous Wigner function, $\Theta(n;t)$. On the other hand, we can also start from a sharp angular momentum state and calculate the Wigner function. The time sequence of this Wigner function, $\rho_w(m,n;t_0)=\delta^{[N]}_{m,k}$, is shown in figure 4 for $N_p=12$, $\chi=0.5$ as in figure 2.

As a special feature of the time evolution of the angle probability distributions we observe from figure 3 that, for small χ, it is dominated by the contribution of the J_z term, the other term only acts as a small perturbation. In this case, the distribution evolves merely by jumping from

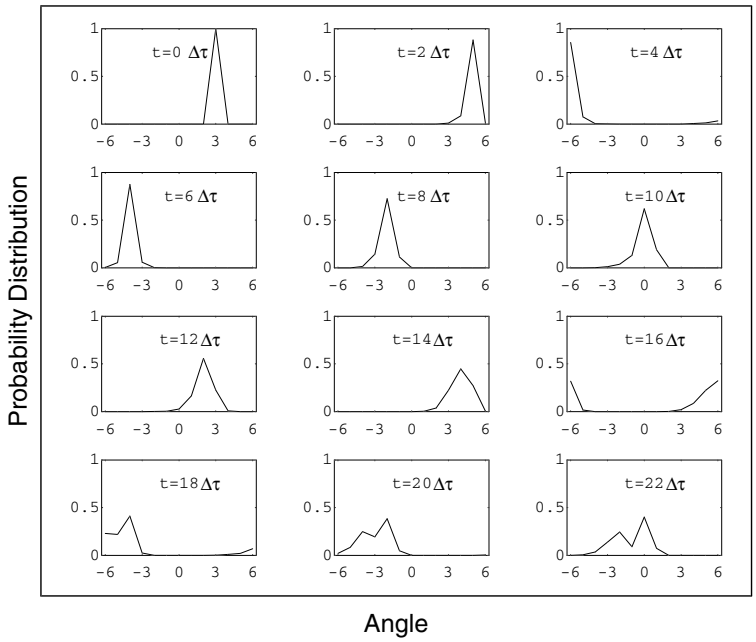

Figure 3. Time evolution of the angle distribution probability, extracted from the Wigner function given in figure 2. The angle axis is in units of $2\pi/N$. The solid line is only given as a guide to the eye.

an angle state to the next one cyclically. At the same time, we observe that, due to the small coupling, a small part of the total probability is being distributed among the close-neighbour states as time goes on, until a fragmentation of the probability distribution is observed around $t = 18 \sim 20\Delta\tau$. This is an indication that a reflection (and correspondently a transmission) occurs at the point $k = -\frac{N_p}{2}$, which, due to the periodic boundary conditions, is identified with $k = \frac{N_p}{2}$.

Again, as can be seen from figure 1, the energy spectrum changes as we increase χ, leading to an almost colapse of the two higher states (and correspondently, by symmetry, to the two lower states) for finite χ. Figure 5 shows the time sequence of the Wigner function associated to the sharp angle state now calculated for $N_p = 12$ and $\chi = 2.0$ and $k = 3$ as in figure 2. Similarly to figure 3, we now have figure 6.

In this case the χ term in the Hamiltonian is no longer just a perturbation, and the time evolution of the angle probability distributions shows strong deviations in comparison with the previous case. First of all, it can be seen that the strong coupling (induced by the χ term) among the angular states leads to a new feature in the time evolution, namely, figure 6 draws our attention to secondary peaks which appear right at the first time step, in contrast to the small-χ case. These peaks depend crucially on the details of the energy spectrum at the particular value of χ, and are direct manifestations of the strong couplings between the corresponding states; in fact, the appearance of these peaks again suggests the behaviour of reflected components on a potential barrier. At the same time, we see that there also appears the equivalent to a transmitted component of the distribution. Therefore, in the time evolution of the angle probability distribution, reflections and transmissions clearly show up.

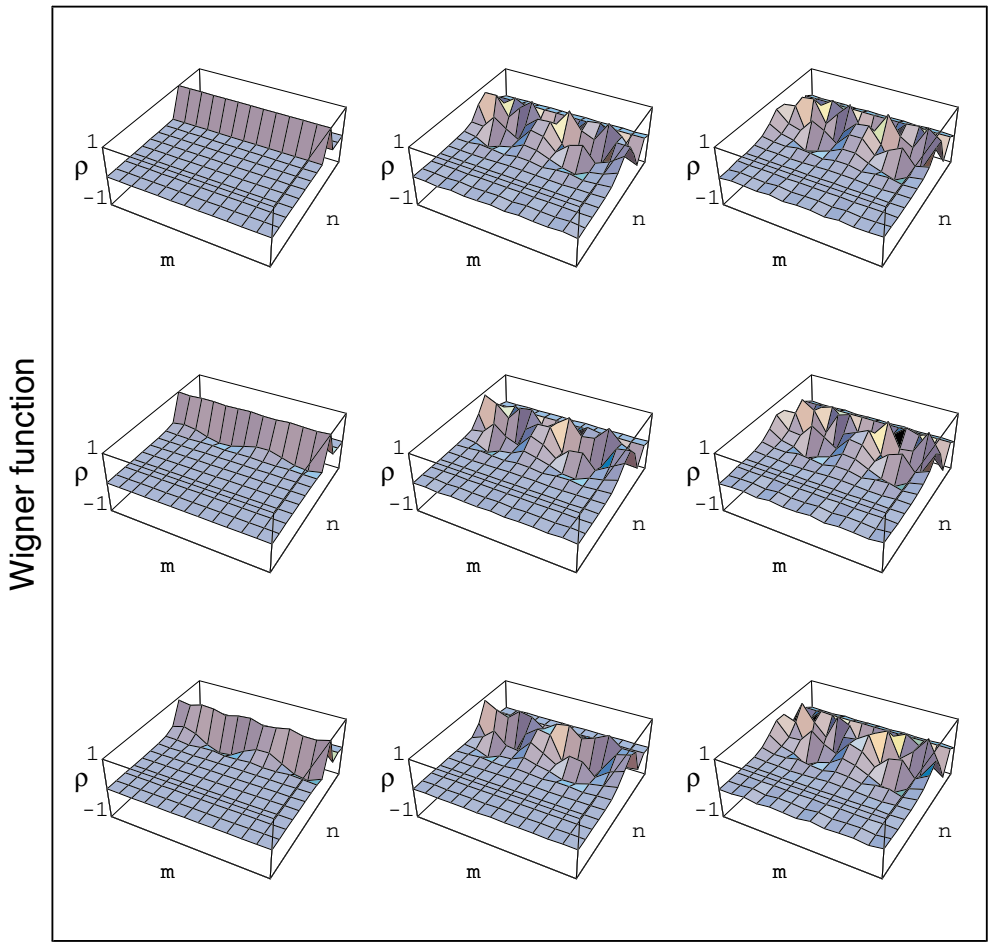

Figure 4. Time evolution of the Wigner function, $\rho_w(m, n; t_0) = \delta^{[N]}_{m,k}$ (angular momentum sharp), for $N_p = 12$ and $\chi = 0.5$. The initial condition is $k = 3$. Other features as in figure 2.

A second aspect must be emphasized for $\chi = 2$ if we compare the time evolution of the angle probability distribution as shown before, figure 6, with that depicted in figure 8, where we have now considered the Wigner function at $t = 0$ for a different initial condition, namely $k = -3$, as seen in figure 7. The time evolution clearly shows that the angle probability distribution fragments into two peaks as it passes through $k = 0$, clearly suggesting that a potential barrier could be present there, contrary to the $\chi = 0.5$ case where no fragmentation was found for the same initial conditions. All these results strongly motivate us to conceive a potential function, associated to this fermionic/quasi-spin system, which must present barriers—whose heights are functions of χ—with maxima at $k = \pm\frac{N_p}{2}, 0$ for increasing χ. We have carried out numerical calculations which indicate that the barrier at $k = 0$ appears for $\chi \gtrsim 1.0$.

In order to test the existence of such a suggested potential and further discuss its features, we will show a connection between the matrix representing the Hamiltonian in the discrete phase space with a semiclassical continuous description of the Lipkin model in the following section.

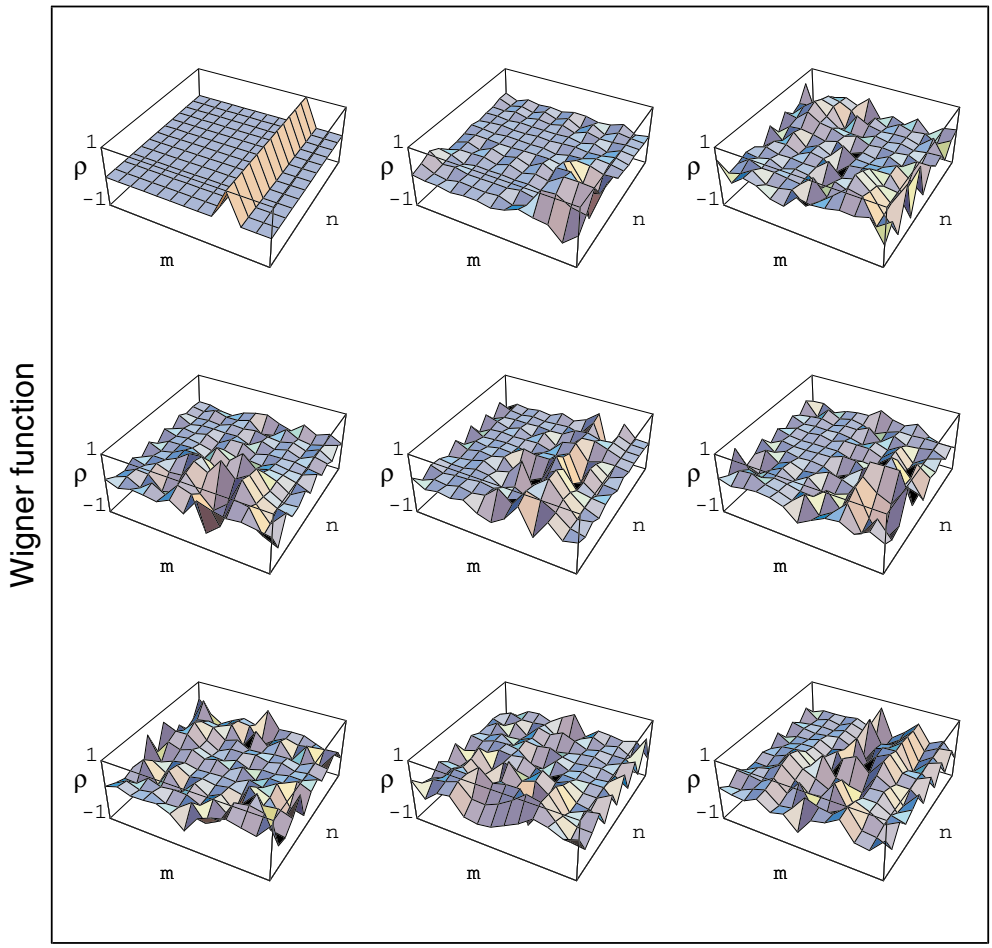

Figure 5. Time evolution of the Wigner function, $\rho_w(m, n; t_0) = \delta^{[N]}_{n,k}$ (angle sharp), for $N_p = 12$ and $\chi = 2.0$. The initial position is $k = 3$. Other features as in figure 2.

4. The connection with a continuous semiclassical representation

It has been long proposed that a $SU(2)$ coherent-state-based description can be used to represent the Lipkin Hamiltonian in terms of one continuous angle variable [28], namely

$$|\phi\rangle = \cos^{N_p}\left(\frac{\phi}{2}\right)\exp\left(\tan\frac{\phi}{2}J_+\right)|0\rangle \tag{27}$$

where $|0\rangle$ is the vacuum of the angular momentum operator. This state is not orthonormalized, thus giving an overlap kernel of the form

$$\langle\phi'|\phi\rangle = \cos^{N_p}\left(\frac{\phi' - \phi}{2}\right). \tag{28}$$

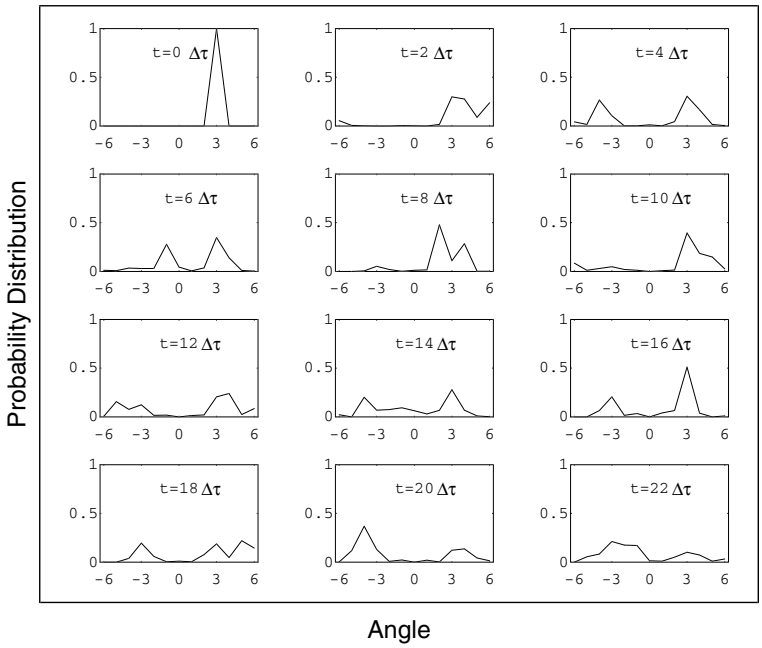

Figure 6. Time evolution of the angle distribution probability, extracted from the Wigner function given in figure 5. Other features as in figure 3.

If we define the new variables $\varphi = \frac{(\phi+\phi)}{2}$ and $\theta = \phi - \phi$, the Lipkin Hamiltonian can be transformed into an energy kernel which reads

$$\langle\phi'|H|\phi\rangle = H(\varphi,\theta) = -\frac{\epsilon N_p}{2}\cos^{N_p}\left(\frac{\theta}{2}\right)\left\{\cos(\varphi)\cos^{-1}\left(\frac{\theta}{2}\right) + \frac{\chi_h}{2}\left[\cos^{-2}\left(\frac{\theta}{2}\right)1+\sin^2(\varphi)) - 1\right]\right\} \tag{29}$$

where now $\chi_h = \chi(N_p - 1)/N_p$, which differs from the interaction parameter we have introduced in the previous sections.

It is interesting to observe that we can pass from this nonorthogonal continuous representation onto a new discrete orthonormalized one if we find a transformation that diagonalizes the overlap kernel, equation (28) [29]. This can be directly accomplished by a Fourier transformation:

$$\int_{-\pi}^{\pi}\langle\phi' \mid \phi\rangle u_m(\phi')\,\mathrm{d}\phi' = \lambda_m u_m(\phi) \tag{30}$$

where the eigenfunctions and eigenvalues are

$$u_m(\phi) = \frac{\exp(\mathrm{i}m\phi)}{\sqrt{2\pi}} \tag{31}$$

$$\lambda_m = \int_{-\pi}^{\pi}\cos^{N_p}\left(\frac{\phi}{2}\right)\exp(\mathrm{i}m\phi)\,\mathrm{d}\phi = \frac{2\pi N_p!}{2^{N_p}(\frac{N_p}{2}+m)!(\frac{N_p}{2}-m)!} \tag{32}$$

respectively with $-\frac{N_p}{2} \leqslant m \leqslant \frac{N_p}{2}$. This diagonalization gives a set of $N = N_p + 1$ orthonormalized states defining a basis in the multiplet we are interested in (which coincides

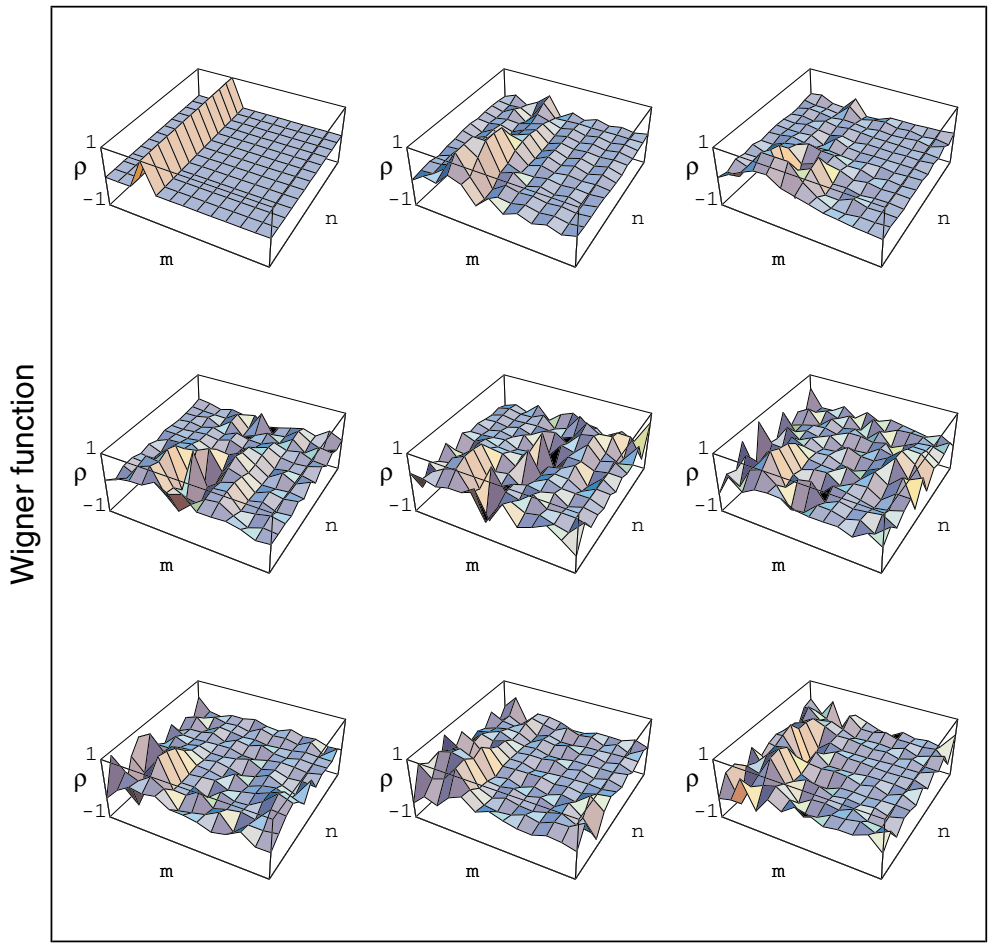

Figure 7. Time evolution of the Wigner function, $\rho_w(m, n; t_0) = \delta^{[N]}_{n,k}$ (angle sharp), for $N_p = 12$ and $\chi = 2.0$. The initial position is $k = -3$. Other features as in figure 2.

with the ground state multiplet we discussed before), with eigenvalues λ_m. If we project the Lipkin energy kernel, written in terms of continuous angle variables, into these angular momentum basis states, we are led to

$$H(m, m') = \int_{-\pi}^{\pi}\int_{-\pi}^{\pi} \exp[\mathrm{i}\varphi(m' - m)] \exp\left[-\mathrm{i}\frac{\theta}{2}(m' + m)\right] \frac{H(\varphi, \theta)}{\sqrt{\lambda_m \lambda_{m'}}} \frac{\mathrm{d}\varphi\, \mathrm{d}\theta}{2\pi} \tag{33}$$

whose analytic expression is

$$\begin{aligned} H(m, m') = \frac{-\epsilon N_p}{4\pi\sqrt{\lambda_m \lambda_{m'}}} \Bigg\{ & \frac{2\pi^2 (N_p - 1)! \delta_{m', m\pm 1}}{2^{N_p - 1}\Gamma(\frac{N_p+1}{2} - \frac{m'}{2} - \frac{m}{2})\Gamma(\frac{N_p+1}{2} + \frac{m'}{2} + \frac{m}{2})} \\ & + \frac{\chi_h}{2}\Bigg[\frac{(3\pi\delta_{m',m} - \frac{\pi}{2}\delta_{m',m\pm 2})2\pi(N_p - 2)!}{2^{N_p-2}\Gamma(\frac{N_p}{2} - \frac{m'}{2} - \frac{m}{2})\Gamma(\frac{N_p}{2} + \frac{m'}{2} + \frac{m}{2})} \\ & - \frac{4\pi^2 N_p! \delta_{m',m}}{2^{N_p}\Gamma(\frac{N_p}{2} - \frac{m'}{2} - \frac{m}{2} + 1)\Gamma(\frac{N_p}{2} + \frac{m'}{2} + \frac{m}{2} + 1)}\Bigg]\Bigg\}. \end{aligned} \tag{34}$$

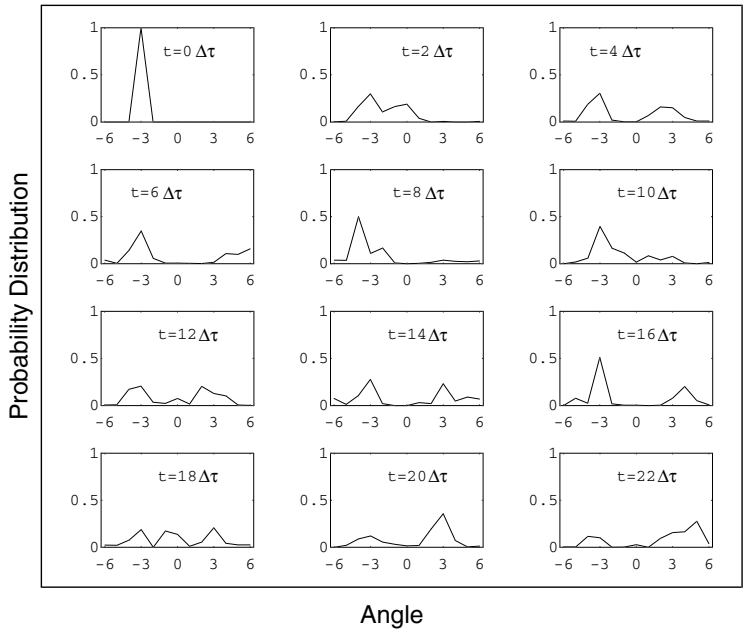

Figure 8. Time evolution of the angle distribution probability, extracted from the Wigner function given in figure 7. Other features as in figure 3.

The diagonalization of this matrix gives the exact spectrum of the Lipkin Hamiltonian, as expected. Thus, the Lipkin Hamiltonian can be directly represented in either the angle (semiclassical) or in the angular momentum description as well.

Since the angular momentum space is characterized by a finite set of states, we are guided to obtain a new discrete representation of the Lipkin Hamiltonian, namely, the *discrete angle representation* associated to the angular momentum one through a discrete Fourier transform, namely,

$$H(k,k') = \sum_{m=-\frac{N-1}{2}}^{\frac{N-1}{2}} \sum_{m'=-\frac{N-1}{2}}^{\frac{N-1}{2}} \frac{\exp(\mathrm{i}m\theta_k)}{\sqrt{N}} H(m,m') \frac{\exp(-\mathrm{i}m'\theta_{k'})}{\sqrt{N}} \tag{35}$$

where θ_k now labels the discrete angle variable, and $\theta_k = \frac{2\pi k}{N}$.

The final entangled matrix of the energy kernel in this discrete angle representation does not allow us a direct comparison with equation (29), which is written in terms of the continuous angle. However, it is possible to extract additional information about the fermionic/quasi-spin system, if we realize that the zeroth moment of this matrix, with respect to the variable $\theta_k - \theta_{k'}$, represents a potential function (of a discrete angular variable) in the variable $(\theta_k + \theta_{k'})/2$. In order to implement this approach, let us define

$$\theta_k - \theta_{k'} = u \tag{36}$$

and

$$\theta_k + \theta_{k'} = 2v. \tag{37}$$

Due to the periodicities of the functions involved, we must only consider the interval for the summation over k as $-\frac{N-1}{2} \leqslant k \leqslant \frac{N-1}{2}$. Furthermore, in order to emphasize the

angular character of this discrete variable we will consider that range to be defined instead as $-\frac{N-1}{N}\pi \leqslant u \leqslant \frac{N-1}{N}\pi$, being the steps of this angular variable $\Delta u = \frac{2\pi}{N}$.

In this form, the zeroth moment will be calculated as

$$M_0(v) = \sum_{u=-\frac{N-1}{N}\pi}^{\frac{N-1}{N}\pi} \frac{\Delta u}{2\pi} \sum_{m,m'=-\frac{N_p}{2}}^{\frac{N_p}{2}} \int_{-\pi}^{\pi}\int_{-\pi}^{\pi} \frac{\exp[\mathrm{i}(v-\varphi)(m-m')]}{2\pi\sqrt{\lambda_m \lambda_{m'}}} \times \exp\left[\mathrm{i}(u-\theta)\frac{(m'+m)}{2}\right] H(\varphi,\theta)\,\mathrm{d}\varphi\,\mathrm{d}\theta. \tag{38}$$

Defining the new variables $r = m' - m$ and $s = (m'+m)/2$, and using the general result

$$\sum_{m=-\frac{N_p}{2}}^{\frac{N_p}{2}} \sum_{m'=-\frac{N_p}{2}}^{\frac{N_p}{2}} = \sum_{r=-N_p}^{-1} \sum_{s=-N_p-r}^{N_p+r} + \sum_{r=1}^{N_p} \sum_{s=r-N_p}^{N_p-r} + \sum_{r=0,s=-N_p}^{N_p} \tag{39}$$

where the summations over s are restricted to run only over even/odd values depending if r is even/odd, we can perform all the integrals and summations. Therefore, that expression gives us the discrete potential function associated to the Lipkin model for the angular variable v.

Now, in order to study the behaviour of the fermions/quasi-spins in the Lipkin model for large N_p (or correspondently for large dimensional spaces), and the associated behaviour of the potential function, we have to discuss the corresponding limits for the summations. First, let us consider the sum in u. Using the change of variables we have introduced before, we see that it is written as

$$\sum_{u=-\frac{N-1}{N}\pi}^{\frac{N-1}{N}\pi} \frac{\Delta u}{2\pi} \exp\left[\mathrm{i}\left(\frac{m'+m}{2}\right)u\right] \tag{40}$$

which, for large N, can be given by the integral

$$\int_{-\pi}^{\pi} \exp\left[\mathrm{i}\frac{ul}{2}\right]\mathrm{d}u = \begin{cases} 0 & \text{if} \quad l = \text{even} \neq 0 \\ 2\pi & \text{if} \quad l = 0 \\ \dfrac{4}{l}(-1)^j & \text{if} \quad l = \text{odd} \quad l = 2j+1. \end{cases} \tag{41}$$

With these results, we end up with

$$\frac{M_0(v)}{\epsilon} = \frac{N_p\chi_h}{4} - \frac{N_p^2\chi_h}{4(N_p-1)}\left[\frac{3}{2} - \cos(2v)\frac{(N_p+2)}{2N_p}\right] - \frac{\cos(v)}{2\pi}\sum_{r=-\frac{N}{2}}^{\frac{N}{2}-1} \frac{(-1)^{r+1}}{2r+1}\sqrt{\left(\frac{N_p}{2}+r+1\right)\left(\frac{N_p}{2}-r\right)}. \tag{42}$$

For $N \gg 1$, we see that

$$\frac{N_p\chi_h}{4} - \frac{3N_p^2\chi_h}{8(N_p-1)} \to -\frac{\chi_h}{8}(N_p+3) \tag{43}$$

$$\frac{N_p\chi_h(N_p+2)}{8(N_p-1)}\cos(2v) \to \frac{\chi_h(N_p+3)}{8}\cos(2v) \tag{44}$$

and

$$\cos(v)\sum_{r=-\frac{N}{2}}^{\frac{N}{2}-1} \frac{(-1)^{r+1}}{2r+1}\sqrt{\left(\frac{N_p}{2}+r+1\right)\left(\frac{N_p}{2}-r\right)} \to -(N_p-1)\frac{\pi}{4}\cos(v). \tag{45}$$

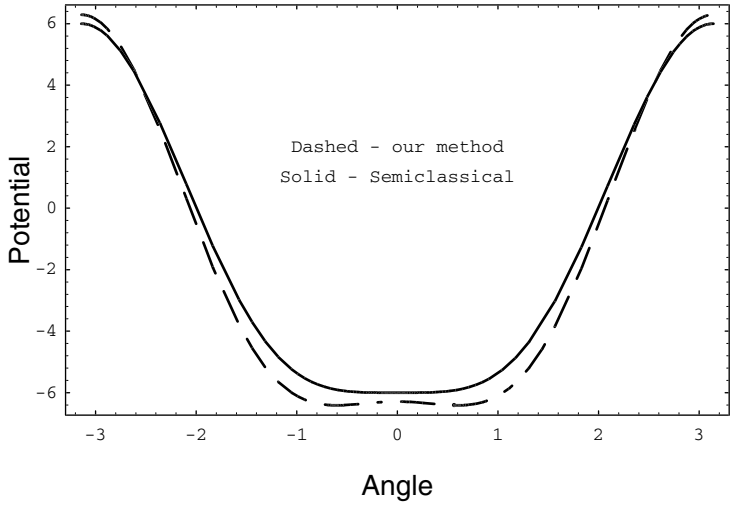

Figure 9. Potential function for $N_p = 12$ and $\chi_h = 1.0$. The dashed curve was obtained from our expression (the line is only provided as a guide to the eye), and the solid line corresponds to the semiclassical approach.

Therefore, when $N \gg 1$, the final form for the potential is

$$\frac{M_0(v)}{\epsilon} = -\frac{(N_p - 1)}{2}\cos(v) - \frac{\chi_h}{8}(N_p + 3) + \frac{\chi_h(N_p + 3)}{8}\cos(2v) \tag{46}$$

which can be rewritten as

$$V(v) = -\frac{(N_p - 1)}{2}\cos(v) - \frac{\chi_h(N_p + 3)}{4}\sin^2(v). \tag{47}$$

It is interesting to observe that this result coincides with that obtained by Holzwarth in his generator coordinate treatment for the Lipkin model [28], while here, alternatively, the result was obtained as the limiting case of large N. This fact, however, can be completely understood if we realize that the Lipkin model attains a classical limit when $N \to \infty$, in the sense that quantum dynamics then becomes the classical dynamics [30]. Figure 9 shows the form of the potential function for $N_p = 12$ and $\chi_h = 1.0$, using our expression and the coherent-state-based semiclassical approach.

5. Conclusions

In this paper we have drawn our attention to the time evolution of the Lipkin model consisting of a finite number of fermions. Due its inherent $SU(2)$ algebraic structure, it has been shown that this model can also be seen as a quasi-spin system. As such, it can be treated within the framework of discrete phase spaces, as has been discussed in the past. This model consists basically of a J_z term disturbed by a term, which is controlled by a strength parameter χ, that couples the states in the finite-energy multiplet; as that parameter increases, the coupling term dominates. In this case, it can be seen that the energies change from a pure J_z spectrum to a strongly distorted one, when a degeneracy occurs for $\chi \to \infty$. In addition to its well known discrete symmetries, this model also exhibits some interesting features when described in terms of discrete angle and action variables. Here we have focused our attention in the discrete phase

space description of the Lipkin model. The discrete von Neumann–Liouville time-evolution equation for this system, which is written in terms of discrete angle and action variables, was exhibited, and the series governing the continuous time evolution of the associated Wigner function was written explicitly, due to the fact that the mapped Hamiltonian for the Lipkin model can be explicitly obtained.

The numerical techniques for calculating the time evolution of the Wigner function and the discrete angle and angular momentum distributions were implemented and the results were obtained in such a form to exhibit the main features of the system behaviour when the parameter χ increases. The change in the energy spectrum clearly reveals itself in the change of the time-evolution pattern of the probability distributions.

First we note that, for small χ, the angle probability distribution just evolves in time by jumping from one site to its neighbour, while the distribution slowly widens due to the weak coupling. After a time of the order of 18–20 $\Delta\tau$, the angle probability distribution breaks into two pieces when it crosses the borderline of the angle domain, namely at $k = \pm 2\pi(N-1)/N$. If we increase χ we note that new features appear in the angle probability distribution. Besides being an indication of strong correlations among the states, these effects are associated to the diminishing value of the energy gap occurring for high values of χ. In particular, we note that the angle distribution breaks within the first time step, and, as the time goes on, secondary peaks appear. This is direct evidence of reflections and transmissions through a potential barrier that must be located at $k = \pm 2\pi(N-1)/N$. In order to test the potential form, we have performed the time evolution of the angle probability distribution which, at $t = 0$, is located at $k = -3$; in this way, it must pass through $k = 0$ just in its initial time steps. We observe that a fragmentation of the probability distribution also occurs at $k = 0$, indicating that the potential function must present a maximum at this point as χ increases. Although we do not have a genuine ground state second-order phase transition in this case (which only occurs for $N \to \infty$, when $\chi_c \to 1$), the time evolution of the angle probability distribution reflects the behaviour of the energy gap. The direct conclusion from this result is that the potential function—written in terms of a discrete angular variable—associated to the finite-dimensional system must present barriers at those mentioned points; the height of the central bump depends on the strength of the coupling constant χ. In this form, we interpret the fragmentation of the probability distributions as a tunnelling effect in which a transmitted component is found in connection with a reflected one.

Finally, we have shown a method to extract such a discrete potential function from a discrete Hamiltonian kernel. In fact we have used the result that the discrete potential function is the zeroth moment of the nonlocal Hamiltonian kernel written in terms of the discrete angular variable. It is then a direct task to establish a connection between the discrete phase space treatment for the Lipkin model and a semiclassical one based on a particular version of a $SU(2)$ coherent state, presented some time ago within the context of a generator coordinate method, when $N_p \to \infty$. To this aim, we had to adapt the form of the Lipkin Hamiltonian in order to compare both treatments in the limit of a great number of fermions/quasi-spins by redefining the coupling constant. In that limit, the main result is that we can extract a potential function of a continuous angle variable from the original discrete treatment, and it will coincide with the potential extracted from the generator coordinate method. At the same time, it was also possible to compare the results for the two versions of the potential function even for a finite number of fermions/quasi-spins. It is interesting to observe that for $\chi_h < 1$ our potential displays a single minimum at $\theta = 0$, while for $\chi_h > 1$ it shows two minima at $-\pi < \theta_1 < 0$, $0 < \theta_2 < \pi$, and one maximum at $\theta = 0$. In this case, with this redefined coupling constant, a discussion of the Lipkin Hamiltonian based on our potential function of a discrete variable also supports the interpretation of a ground state

phase transition, and we can therefore interpret the transmissions and reflections found in the time evolution of the discrete Wigner function as a tunnelling effect through those potential barriers.

Acknowledgments

M Ruzzi is supported by Fundação de Amparo à Pesquisa do Estado de São Paulo, FAPESP, and D Galetti is partially supported by Conselho Nacional de Desenvolvimento Científico e Tecnológico, CNPq, Brazil.

References

[1] Weyl H 1978 *The Theory of Groups and Quantum Mechanics* (New York: Dover)
[2] de Groot S R and Suttorp L G 1972 *Foundations of Electrodynamics* (Amsterdam: North-Holland)
[3] Hillery M, O'Connell R F, Scully M O and Wigner E P 1984 *Phys. Rep.* C **106** 121
[4] Balazs N L and Jennings B K 1984 *Phys. Rep.* C **104** 347
[5] Kim Y S and Noz M E 1991 *Phase Space Picture of Quantum Mechanics* (Singapore: World Scientific)
[6] Lee H W 1995 *Phys. Rep.* C **259** 147
[7] Ozório de Almeida A M 1998 *Phys. Rep.* C **295** 265
[8] Wooters W K 1987 *Ann. Phys.* **176** 1
[9] Galetti D and de Toledo Piza A F R 1988 *Physica* A **149** 267
[10] Cohendet O, Combe Ph, Sirugue M and Sirugue-Collin M 1988 *J. Phys. A: Math. Gen.* **21** 2875
[11] Zak J 1989 *J. Math. Phys.* **30** 1591
[12] Zak J 1989 *J. Math. Phys.* **39** 694
[13] Galetti D and de Toledo Piza A F R 1992 *Physica* A **186** 513
[14] Kasperkovitz P and Peev M 1994 *Ann. Phys., NY* **230** 21
[15] Hakioğlu T 1998 *J. Phys. A: Math. Gen.* **31** 6975
[16] Luis A and Peřina J 1998 *J. Phys. A: Math. Gen.* **31** 1423
[17] Chudnovsky E M and Tejada J 1998 *Macroscopic Tunnelling of the Magnetic Moment* (Cambridge: Cambridge University Press)
[18] Leonhardt U 1995 *Phys. Rev. Lett.* **74** 4101
Leonhardt U 1996 *Phys. Rev.* A **53** 2998
[19] Vourdas A 1990 *Phys. Rev.* A **41** 1653
Vourdas A 1991 *Phys. Rev.* A **43** 1564
[20] Galetti D and Ruzzi M 1999 *Physica* A **264** 473
[21] Lipkin H J, Meshkov N and Glick A J 1965 *Nucl. Phys.* **62** 188
[22] Gilmore R and Feng D H 1978 *Nucl. Phys.* A **301** 189
[23] Kan K K, Griffin J J, Lichtner P C and Dworzecka M 1979 *Nucl. Phys.* A **332** 109
[24] Shankar R 1980 *Phys. Rev. Lett.* **45** 1088
[25] Klein A and Li C T 1981 *Phys. Rev. Lett.* **46** 895
[26] Galetti D and de Toledo Piza A F R 1995 *Physica* A **214** 207
[27] Schwinger J 1960 *Proc. Natl Acad. Sci. USA* **46** 570, 893, 1401
Schwinger J 1961 *Proc. Natl Acad. Sci. USA* **47** 1075
[28] Holtzwarth G 1973 *Nucl. Phys.* A **207** 545
[29] de Toledo Piza A F R, de Passos E J V, Galetti D, Nemes M C and Watanabe M M 1977 *Phys. Rev.* C **15** 1477
[30] Jaffe L 1982 *Rev. Mod. Phys.* **54** 497